UNIFAC Model for Ionic Liquid-CO_2 Systems

Zhigang Lei, Chengna Dai, Wei Wang, and Biaohua Chen
State Key Laboratory of Chemical Resource Engineering, Beijing University of Chemical Technology, Box 266, Beijing 100029 China

DOI 10.1002/aic.14294
Published online November 26, 2013 in Wiley Online Library (wileyonlinelibrary.com)

The new group binary interaction parameters of UNIFAC model (a_{nm} and a_{mn}) between CO_2 and 22 ionic liquid (IL) groups were obtained by means of correlating the solubility data of CO_2 in pure ILs at different temperatures (>273.2 K). We measured the CO_2 solubility at low temperatures down to 243.2 K in pure ILs, i.e., $[OMIM]^+[BF_4]^-$ and $[OMIM]^+[Tf_2N]^-$, and their equimolar amount of mixture, in order to fill the blank of solubility data at low temperatures and also to justify the applicability of UNIFAC model over a wider temperature range. It was verified that UNIFAC model can be used for predicting the CO_2 solubility in pure ILs and in the binary mixture of ILs both at high (>273.2 K) and low temperatures (<273.2 K) effectively, as well as identifying the new structure–property relation. This is the first work to extend the UNIFAC model to IL-CO_2 systems. © 2013 American Institute of Chemical Engineers
AIChE J, 60: 716–729, 2014
Keywords: UNIFAC model, CO_2 solubility, ILs, low temperatures, structure, property relation

Introduction

In recent years, the emissions of carbon dioxide (CO_2) are increasing, leading to a series of environmental problems. Therefore, carbon capture and storage (CCS) becomes an important issue for an environmentally benign and sustainable development. Ionic liquids (ILs) as novel green solvents have unique peculiarities such as their almost negligible vapor pressure, high thermal and chemical stability, tunable chemical structures, and low-melting point, which make them a promising alternative for the replacement of volatile organic solvents in gas absorption and separation.[1–4] However, in some cases, e.g., the syngas purification for Fischer-Tropsch (FT) synthesis and the production of NH_3, the content of CO_2 for syngas is usually limited to ppm level (2 ppm to 3% by volume depending on the type of synthesis) before reaction,[5] and the absorption process operating above room temperature could not meet the requirement because the solubility of CO_2 in ILs decreases with increasing temperature. Thus, the solubility of CO_2 in ILs at low temperatures down to 243 K as in the world-famous Rectisol process[6] using methanol as separating agent has to be determined to provide fundamental knowledge for developing gas separation techniques unitizing the unique properties of ILs.

Unfortunately, although there are a large number of publications on the solubility of CO_2 in pure ILs at high temperatures (>273.2 K),[7–22] the investigation on the solubility of CO_2 in pure ILs at low temperatures (<273.2 K) has not been reported by far. Therefore, in this work, we decided to measure the CO_2 solubility at low temperatures down to 243.2 K in two common ILs as the representatives, i.e., $[OMIM]^+[BF_4]^-$ and $[OMIM]^+[Tf_2N]^-$. However, it is tedious and time-consuming to measure the solubility of CO_2 in all ILs at low temperatures through experiments one by one. Therefore, it is highly desirable to develop an effective and efficient predictive model so as to reduce the amount of experimental work.

Several predictive thermodynamic models, e.g., regular solution theory (RST),[23–26] the series of statistical associating fluid theory (SAFT) EOS[27–30] (e.g., perturbed-chain SAFT (PC—SAFT), soft-SAFT, heterosegmented-SAFT, and SAFT-γ), and COSMO—RS (conductor-like screening model for real solvents)[31–33] have been proposed for IL—CO_2 systems. The formulations of SAFT EOS are much complicated and a number of pure component parameters and cross-association binary parameters have to be concerned, thus limiting their engineering application. The COSMO—RS model is a novel method for predicting thermodynamic properties of pure and mixed liquids on the basis of unimolecular quantum chemical calculations for the respective individual molecules or ions. As *a priori* prediction method, it requires molecular structure as the only information, regardless of any experimental data. Some researchers[32] have used the COSMO—RS model to predict the CO_2 solubility in ILs, and found that the COSMO—RS model sometimes cannot predict the correct trend in the order of CO_2 solubility in comparison with experimental data. Thus, there is a great risk of producing very poor predictions when using the COSMO—RS model. On the other hand, the RST model offers a simple method to predict the gas solubility in ILs at low pressures and near ambient temperature. As a semiquantitative model, a few solubility parameters for ILs are included only, and some model parameters are even related to a particular temperature. Thus, it

Additional Supporting Information may be found in the online version of this article.

Correspondence concerning this article should be addressed to Z. Lei at leizhg@mail.buct.edu.cn (or)B. Chen at chenbh@mail.buct.edu.cn.

cannot be extrapolated to other temperatures or high pressures.

However, the classic UNIFAC model has recently received broad attention for the prediction of thermodynamic properties of systems with ILs because its formulation is simple, and can be directly incorporated into such famous simulation programs as ASPEN PLUS and PROII to establish equilibrium stage (EQ) and nonequilibrium stage (NEQ) models.[34–36] Based on the original UNIFAC model established by Gmehling,[37–42] we successfully extended the UNIFAC model to the IL-containing systems, with 45 main groups and 77 subgroups for ILs reported in our previous works.[43,44] However, the binary interaction parameters between IL and CO_2 groups have not yet been included, and, thus, should be considered to meet the increasing requirements put forward by chemical engineers engaged in gas separation.

It was known that the solubility of CO_2 in ILs increases with increasing the number of carbon atoms in the alkyl chain on the cation; however, the selectivity relative to other gases often decreases simultaneously. Therefore, the binary mixture of ILs, which is commercially available, can serve as the separating agents to tune the separation ability conveniently, resulting in a desirable solubility and selectivity for capturing CO_2. However, the investigation on the solubility of CO_2 in a binary mixture of ILs is still scarce. Baltus et al.[45] first reported the Henry's law constant of CO_2 in the mixture of 58 mol % $[OMIM]^+[Tf_2N]^-$ and 42 mol % $[C_8F_{13}MIM]^+[Tf_2N]^-$ at 298.2 K and pressure close to 1 bar, which lies between the Henry's law constants in pure $[OMIM]^+[Tf_2N]^-$ and $[C_8F_{13}MIM]^+[Tf_2N]^-$. We previously[46] measured the solubility behaviors of CO_2 in the mixture of $[EMIM]^+[BF_4]^-$ and $[OMIM]^+[Tf_2N]^-$, as well as in the mixture of $[BMIM]^+[BF_4]^-$ and $[OMIM]^+[Tf_2N]^-$ at different mixed concentrations above room temperatures (313.2 and 333.2 K) and pressures up to 60.0 bar. Finotello et al.[47] measured the solubility behaviors of CO_2, CH_4, and N_2 gases in the binary mixtures of imidazolium-based room-temperature ionic liquids (RTILs) using $[EMIM]^+[Tf_2N]^-$ and $[EMIM]^+[BF_4]^-$ at 40°C and low pressures (close to 1 atm). The solubility data of CO_2 in a mixture containing a fixed mole ratio of 49.98% $[EMIM]^+[Ac]^-$ to 50.02% $[EMIM]^+[TFA]^-$ using a gravimetric microbalance at three temperatures (298.1, 323.1, and 348.1 K) and pressures up to about 2.0 MPa were measured by Shiflett and Yokozeki,[48] showing a combination of chemical and physical absorptions. Furthermore, it was found that CO_2 solubility at a fixed pressure can be well predicted by a so-called lever rule which is based on the mole fraction average of individual ILs. However, the solubility data of CO_2 in the binary mixtures of ILs at low temperatures (<273.2 K) have never been reported, and no predictive model has been proposed for estimating the CO_2 solubility in mixed ILs at high pressures. As a result, it is difficult to optimize the IL composition needed to prepare a mixture effective for capturing CO_2 only through experiments without the establishment of predictive models.

Therefore, the focus of this work is on addressing the cogently interesting issues for the UNIFAC model as to (1) extending the group parameters of UNIFAC model between CO_2 and IL groups obtained by means of correlating the experimental data exhaustively collected from literatures at high temperatures (>273.2 K), (2) checking the availability of new group parameters for predicting the solubility of CO_2 in pure ILs at low temperatures (<273.2 K), (3) checking the availability of new group parameters for predicting the solubility of CO_2 in the binary mixtures of ILs from high to low temperatures, and (4) identifying new structure–property relation for CO_2 solubility in ILs by means of the UNIFAC model. In this work, the CO_2 solubility data in $[OMIM]^+[BF_4]^-$, $[OMIM]^+[Tf_2N]^-$, and their equimolar amount of mixture at low temperatures (243.2, 258.2, and 273.2 K) and pressures up to 25 bars were measured so as to justify the applicability of UNIFAC model. The meanings of abbreviations for anions and cations of ILs throughout this article are given online in Supporting Information.

Experimental Section

Materials

The ILs $[OMIM]^+[BF_4]^-$ (purity > 99%, water content < 2000 ppm, and chloride content < 150 ppm in mass fraction) and $[OMIM]^+[Tf_2N]^-$ (purity > 99%, water content <600 ppm, and chloride content < 150 ppm in mass fraction) were purchased from Shanghai ChengJie Chemical Co., Ltd. Before use, they were degassed and dried in a vacuum rotary evaporator at 333.2 K for 48 h to remove traces of water and other volatile impurities. After rotary evaporation, the water contents in $[OMIM]^+[BF_4]^-$ and $[OMIM]^+[Tf_2N]^-$ were less than 200 and 60 ppm, respectively, as determined by Karl-Fischer titration method (SC-6). CO_2 was purchased from Beijing Analytical Instrument Factory with a high purity of 99.995 wt % for experiments without further purification. The mixture containing equimolar amounts of $[OMIM]^+[BF_4]^-$ and $[OMIM]^+[Tf_2N]^-$ was prepared in a cleaned conical flask from the dried pure samples.

Apparatus and procedure

The solubility data of CO_2 in ILs were measured in a low-temperature high-pressure equilibrium cell, which was immersed into a temperature-controlled ethanol bath device for controlling the cooling temperature with a fluctuation of ± 0.1 K. The schematic diagram of this experimental apparatus is shown in Figure 1, which consists of a stainless steel equilibrium cell with constant volume (V_E = 480 mL), a stirring paddle, an ethanol bath, gas manifold, and gas reservoir.

In a typical experiment, a predetermined amount of ILs (m_{IL}) was loaded into the equilibration cell, and the system was purged of the air by vacuum pump (2XZ-1) with all valves (V1–V6) opened. A small amount of gas was charged into the cell in order to replace the residual air, and the operation was repeated several times. With valves (V1 and V2) closed, some CO_2 was introduced into a gas reservoir (3). Then, the valves (V3, V4, V5, and V6) were closed, and the gas reservoir (3) as well as valves (V4 and V5) was taken out to weigh by an electronic balance (CPA 1003S, Sartorius) with an uncertainty of 0.001 g, the weight being recorded as m_1. Afterward, the gas reservoir (3) was connected with valve (V3) again, while keeping the valves (V1, V3, and V4) to the equilibrium cell open, so that a certain amount of CO_2 was introduced into the equilibrium cell in contact with IL. The valves (V1, V3, and V4) were kept closed during the whole phase equilibrium. The gas reservoir as well as valves (V4 and V5) was taken out to weight again, the weight being recorded as m_2. Therefore, the amount of CO_2 gas contained in the equilibrium cell was (m_1 - m_2). The liquid phase was stirred at a speed of about

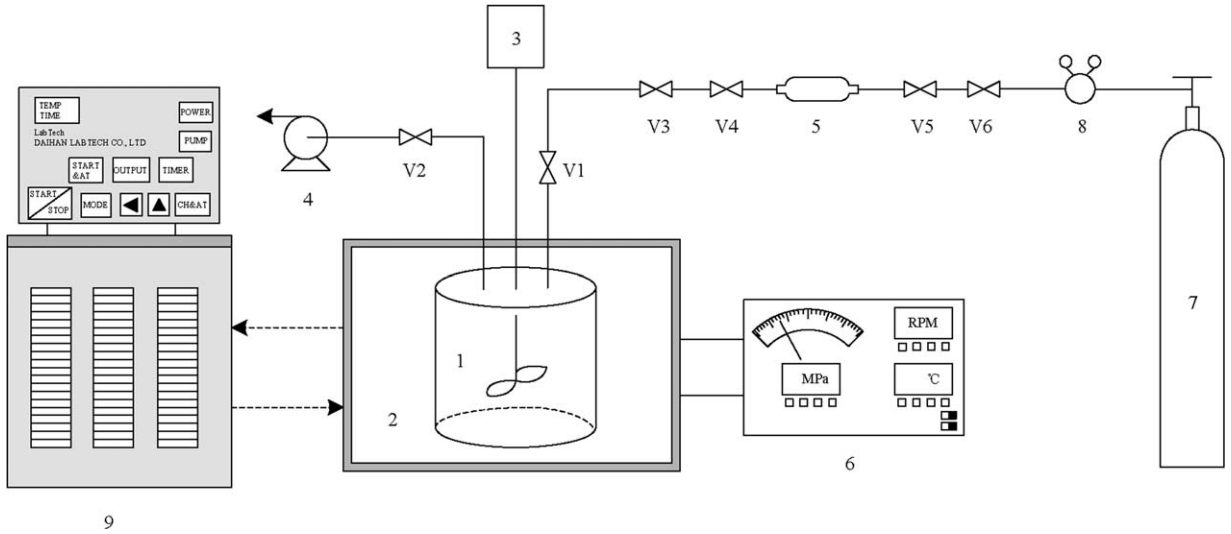

Figure 1. Schematic diagram of the experimental apparatus for measurement of the solubility of CO_2 in ILs at low temperatures.

(1) Equilibrium cell, (2) ethanol bath, (3) stirring paddle, (4) vacuum pump, (5) gas reservoir, (6) pressure and temperature display, (7) CO_2 cylinder, (8) cylinder regulator, and (9) refrigeration compressor.

250 rpm to expedite the gas-liquid equilibrium. The system pressure was measured by a pressure gauge (HQ sensor 1000) with a range of 0–9.999 MPa and an uncertainty of ± 0.001 MPa. It was assumed that gas-liquid equilibrium had been reached until there was almost no pressure change. Each run took about 5 days to ensure sufficient equilibrium time.

Data reduction

The solubility data of CO_2 (1) in pure ILs or binary mixture of ILs were measured in the similar manner as isochoric saturation method using the negligible vapor pressure of ILs, and can be determined by

$$x_1 = \frac{n_{CO_2}}{n_{CO_2} + n_{IL}} = \frac{n_{CO_2}}{n_{CO_2} + m_{IL}/M_{IL}} \quad (1)$$

$$n_{CO_2} = n_{t,CO_2} - n_{g,CO_2} \quad (2)$$

$$n_{t,CO_2} = \frac{m_1 - m_2}{M_{CO_2}} \quad (3)$$

$$n_{g,CO_2} = \frac{V_E - V(T,P)}{V_{m,CO_2}(T,P)} \quad (4)$$

where x_1 is the mole fraction of CO_2 in liquid phase n_{t,CO_2}, n_{g,CO_2} and n_{CO_2} are the total amount of CO_2 introduced into the equilibrium cell, the amount of CO_2 in the gas phase, and the amount of CO_2 dissolved in the liquid phase, respectively n_{IL}, is the total amount of pure ILs or mixed ILs, M is the molecular weight; $V_{m,CO_2}(T,P)$ is the molar volume of CO_2 in gas phase obtained from NIST database (see http://webbook.nist.gov/chemistry/); and $V(T, P)$ represents the total volume of IL/CO_2 mixture in the liquid phase at a given temperature and pressure. The liquid volume correction due to the dissolution of CO_2 was taken into account by a simple mole fraction average for the molar volume &Vtilde;$_m$ as proposed by Lei et al.[46] and Shiflett and Yokozeki[48]

$$\tilde{V}_m(T,P) = \tilde{V}_{IL}(1-x) + \tilde{V}_{CO_2}x \quad (5)$$

which can be rewritten as

$$V(T,P) = V_{IL} + \tilde{V}_{CO_2}n_{CO_2} \quad (6)$$

where $V(T, P)$ is the volume of IL/CO_2 mixture; V_{IL} (= m_{IL}/ρ_{IL}) is the volume of pure ILs determined by the new group contribution method as proposed by Paduszyński and Domańska,[49] with a high accuracy with average absolution relative deviations (AARDs) only 0.53%; and $\tilde{V}_{CO_2}$ is the molar volume of dissolved CO_2 calculated by the Zellner method.[50] Canongia Lopes reported[51] that there would be a positive excess molar volume while mixing two kinds of ILs together, but this value is very small when the two ILs have a common cation. For the mixture of $[BMIM]^+[BF_4]^-$ and $[BMIM]^+[Tf_2N]^-$, the maximum excess molar volume takes only 0.1% of the molar volume of $[BMIM]^+[Tf_2N]^-$. Thus, in this work the effect of excess molar volume is neglected. For the mixed ILs, the density and molecular weight were calculated by using the following mixing rules

$$\rho_{mix} = \frac{\sum_i X_i M_i}{\sum_i \frac{X_i M_i}{\rho_i}} \quad (7)$$

$$M_{mix} = \sum_i X_i M_i \quad (8)$$

where ρ_i is the density of pure ILs (see Supporting Information), and X_i is the mole fraction of IL in the mixture on a CO_2-free basis. In this way, the estimated uncertainty of the solubility measurement in mole fraction was less than 0.006.

To verify the accuracy and reliability of experimental method and apparatus, the solubility of CO_2 in $[HMIM]^+[BF_4]^-$ at 298.2 K and pressures up to 10 bars was measured. The comparison between experimental solubility data and the values coming from literature[36] is given in Supporting Information, with the ARD (average relative deviation) 1.82%.

Thermodynamic Model

Model description

The original UNIFAC model was first proposed by Fredenslund et al.[52] in 1975, as a group-contribution method

combining the solution-of-functional-groups concept with a model for activity coefficients based on an extension of the universal-quasi-chemical theory (UNIQUAC) of liquid mixtures. To apply the UNIFAC model, the IL molecule must first be divided into several separate groups. There are three approaches for the decomposition of IL groups (1) the IL is divided into one cation and one anion groups.[53,54] This approach does not reflect the influence of structural variation of substitutents on the cation or anion on the separation performance, (2) the IL is divided into cation core, anion and several CH_2 or CH_3 groups.[55–58] This approach requires a large number of experimental data used to correlate the group interaction parameters, and (3) the skeleton of cation and anion is treated as a whole, and the alky chain is decomposed into separate CH_2 or CH_3 groups.[36,43,44,59–63] In this approach, ILs are divided into electrically neutral groups, and, thus, the additional Debye-Hückel term accounting for long-range electrostatic contributions can be neglected. As a result, this approach was adopted in this work.

In the UNIFAC model, the activity coefficient expressed as a function of temperature and composition, is composed of two parts, i.e., the combinatorial part and the residual part

$$\ln \gamma_i = \ln \gamma_i^{C} + \ln \gamma_i^{R} \tag{9}$$

where $\ln \gamma_i^{C}$ represents the combinatorial contribution to the activity coefficient, which is caused by the different size and shape of groups, and contains two group parameters R_k and Q_k. The group parameters can be derived from the previous work,[38,43,44,64] or calculated by $R_k = \frac{V \times N_A}{V_{VW}}$ and $Q_k = \frac{A \times N_A}{A_{VW}}$, where N_A is the Avogadro's number (6.023×10^{23} mol^{-1}), V and A are group volume and surface area calculated by the COSMO–RS model, respectively, and V_{VW} and A_{VW} are 15.17 $cm^3 \cdot mol^{-1}$ and 2.5×10^9 $cm^2 \cdot mol^{-1}$, respectively, as suggested by Bondi.[65] $\ln \gamma_i^{R}$ represents the residual contribution, which is essentially due to energetic interaction between groups, and is a function of the group interaction parameters a_{nm} and a_{mn}.

The group interaction parameters (a_{nm} and a_{mn}) between IL group and the main group CH_2 as well as between CO_2 and the main group CH_2 can be found from previous publications.[43,66] Therefore, the group interaction parameters (a_{nm} and a_{mn}) only between IL group and CO_2 are the unknown input parameters, which should be derived by means of correlating the experimental CO_2 solubility data in pure ILs at different temperatures (>273.2 K) and pressures exhaustively collected from other literatures.

Procedure of the estimation of group interaction parameters

For the CO_2 (1) + IL (2) binary system, the gas-liquid equilibrium at low and medium pressure can be described as

$$y_1 P \varphi_1(T, P, y_1) = x_1 \gamma_1 P_1^{s} \tag{10}$$

where x_1 and y_1 represent the mole fractions of CO_2 in liquid and gas phases, respectively; $\varphi_1(T, P, y_1)$ is the gas-phase fugacity coefficient of CO_2 calculated from the equation of state proposed by Span and Wagner;[67] P is the system pressure; P_1^{s} is the saturated vapor pressure of CO_2 calculated by the extrapolated Antoine equation as proposed by Shiflett and Yokozeki;[68] and γ_1 is the activity coefficient of CO_2, which can be calculated by the UNIFAC model. It is noted that the gas phase can be treated as pure CO_2 gas (i.e., $y_1 = 0$) since IL has a negligible vapor pressure.[69]

The average relative deviation (ARD) minimized was adopted as objective function (OF)

$$OF = \frac{1}{N} \sum_{1}^{N} \left| \frac{x_{cal} - x_{exp}}{x_{exp}} \right| \tag{11}$$

where x_{exp} is the experimental CO_2 solubility data exhaustively collected from literatures; x_{cal} is the calculated CO_2 solubility data by the UNIFAC model, and N is the number of data points. In this work, the binary interaction parameters between CO_2 and IL groups were obtained by correlating the solubility data of CO_2 arranged according to the category of ILs having the same skeleton of cation and anion. We are aware that the collected solubility data were measured by different techniques or using the same experimental method but measured by different research groups. In this case, the experimental data, which do not conform to the general structure–property relation, were excluded. It was found that only a few experimental data are suspicious. Meanwhile, most of the experimental data are present on a mole fraction basis except for several solubility data present on a molality (unit: mol $CO_2 \cdot kg^{-1}$ IL) or mole ratio (unit: mol $CO_2 \cdot mol^{-1}$ IL) basis. Herein, these data have to be converted into the uniform mole fraction basis.

The SOLVER function with the optimization algorithm of Newton's central difference in Microsoft Excel 2003 was adopted to correlate the group binary interaction parameters (a_{nm} and a_{mn}) using the solubility data at temperatures of 278–453 K, and pressures of 0.01–971.00 bar. The fitting procedure is similar to our previous publications.[43,44] In this way, the feasible and near-optimal solutions to the regression problem can be reached.

A five-fold cross validation method was applied to estimate the predictive power of UNIFAC model. The solubility data for each kind of IL groups (with the same skeleton of cation and anion) were randomly partitioned into five subsets of data of equal size. Four sets of the data were used as a training set to obtain the binary interaction parameters, and the other one was used as a validation set to check the predictive power of the model. Thus, five models, named as Model 1/5, Model 2/5, Model 3/5, Model 4/5, and Model 5/5, were introduced, and each one contained 1/5 data. The Root Mean Square Error of Approximation (RMSEA) minimized was used to select the optimum values for interaction parameters.

$$\mathrm{RMSEA} = \sqrt{\max\left([(\chi^2/df - 1)/(N-1)], 0\right)} \tag{12}$$

where χ^2 is the chi-square value, df is the degree of freedom, and N is the sample size. MacCallum et al.[70] used the RMSEA values 0.01, 0.05, and 0.08 to indicate excellent, good, and mediocre fits for a model, respectively. However, others have suggested 0.10 as the cutoff for poor fitting models.[71] The group binary interaction parameters (a_{nm} and a_{mn}) between CO_2 and 22 IL groups, as well as the RMSEA values, are listed in Table 1. It can be seen that the RMSEA values in most cases are below 0.08, indicating the applicability of UNIFAC model. The current UNIFAC parameter matrix is illustrated in Figure 2. The kinds of ILs, more than 5400 solubility data points, experimental methods and the corresponding cited literatures are provided in detail in Supporting Information.

Table 1. Group Binary Interaction Parameters α_{mn} and α_{nm} Between CO_2 (m) and IL Group (n) for the UNIFAC Model

Main groups	Models	No. of data points in training set	No. of data points in validation set	α_{mn}	α_{nm}	RMSEA for validation set	RMSEA for all data
[MIM][BF_4]	Model 1/5	620	155	−15.3868	430.5254	0.0595	0.0499
	Model 2/5	620	155	−15.6938	430.4648	0.0453	0.0499
	Model 3/5	620	155	−13.6521	431.0390	0.0530	0.0495
	Model 4/5	620	155	−13.6666	431.0830	0.0475	0.0495
	Model 5/5	620	155	−14.4413	430.7991	0.0410	0.0496
	Optimum values for interaction parameters			−14.4413	430.7991		
[MIM][Tf_2N]	Model 1/5	1467	366	14.5632	81.4726	0.0650	0.0720
	Model 2/5	1466	367	15.2465	78.6457	0.0686	0.0718
	Model 3/5	1466	367	14.5301	80.5347	0.0675	0.0719
	Model 4/5	1467	366	19.4642	75.3566	0.0881	0.0720
	Model 5/5	1466	367	19.0783	75.0256	0.0679	0.0719
	Optimum values for interaction parameters			14.5632	81.4726		
[MIM][PF_6]	Model 1/5	663	165	−60.8959	461.5565	0.0740	0.0652
	Model 2/5	662	166	−59.8836	451.8236	0.0749	0.0656
	Model 3/5	662	166	−66.7409	460.2493	0.0422	0.0666
	Model 4/5	662	166	−64.0534	471.0697	0.0738	0.0652
	Model 5/5	663	165	−67.4639	483.0794	0.0571	0.0653
	Optimum values for interaction parameters			−66.7409	460.2493		
[MIM][TfO]	Model 1/5	283	70	−160.0226	586.3646	0.0985	0.0783
	Model 2/5	282	71	−164.3934	585.5045	0.0909	0.0787
	Model 3/5	283	70	−162.1211	572.3386	0.0628	0.0787
	Model 4/5	283	70	−162.0887	585.6760	0.0669	0.0785
	Model 5/5	282	71	−161.4688	585.7983	0.0663	0.0784
	Optimum values for interaction parameters			−162.1211	572.3386		
[MIM][$MeSO_4$]	Model 1/5	43	11	138.1802	108.9303	0.0349	0.0375
	Model 2/5	43	11	121.1340	93.2455	0.0352	0.0389
	Model 3/5	44	10	138.1776	108.9332	0.0329	0.0375
	Model 4/5	43	11	123.2631	95.0795	0.0518	0.0385
	Model 5/5	43	11	137.2056	108.0240	0.0308	0.0375
	Optimum values for interaction parameters			137.2056	108.0240		
[MIM][$EtSO_4$]	Model 1/5	76	19	313.5971	168.6811	0.0170	0.0252
	Model 2/5	76	19	319.5117	181.8144	0.0108	0.0243
	Model 3/5	76	19	310.4847	162.7083	0.0334	0.0261
	Model 4/5	76	19	402.7670	138.5787	0.0298	0.0249
	Model 5/5	76	19	313.9146	169.4787	0.0314	0.0251
	Optimum values for interaction parameters			319.5117	181.8144		
[MIM][Cl]	Model 1/5	36	9	2693.8036	−68.4551	0.0307	0.0427
	Model 2/5	36	9	2693.8013	−71.0541	0.0596	0.0436
	Model 3/5	36	9	2693.8046	−67.3521	0.0236	0.0423
	Model 4/5	36	9	2693.7995	−73.3449	0.0567	0.0445
	Model 5/5	36	9	2693.8049	−67.3521	0.0361	0.0423
	Optimum values for interaction parameters			2693.8046	−67.3521		
[MIM][$DEPO_4$]	Model 1/5	18	4	228.8579	98.1212	0.0003	0.0004
	Model 2/5	18	4	227.3430	95.4983	0.0005	0.0004
	Model 3/5	17	5	228.8579	98.1212	0.0003	0.0004
	Model 4/5	17	5	227.3430	95.4983	0.0005	0.0004
	Model 5/5	18	4	228.8579	98.1212	0.0003	0.0004
	Optimum values for interaction parameters			228.8579	98.1212		
[MIM][$DMPO_4$]	Model 1/5	10	2	826.9872	1177.0552	0.0002	0.0002
	Model 2/5	9	3	822.2149	1178.0258	0.0001	0.0002
	Model 3/5	9	3	826.8938	1178.4007	0.0003	0.0002
	Model 4/5	10	2	825.4959	1177.7283	0.0001	0.0002
	Model 5/5	10	2	828.5326	1176.3675	0.0001	0.0002
	Optimum values for interaction parameters			825.4959	1177.7283		
[MIM][$MDEGSO_4$]	Model 1/5	33	8	277.7267	179.5194	0.0115	0.0543
	Model 2/5	33	8	276.4652	177.2476	0.0642	0.0550
	Model 3/5	33	8	232.1762	197.9778	0.1034	0.0565
	Model 4/5	33	8	277.2195	178.5498	0.0250	0.0545
	Model 5/5	32	9	277.2967	178.3609	0.0259	0.0546
	Optimum values for interaction parameters			277.7267	179.5194		
[MIM][NO_3]	Model 1/5	83	21	111.2882	519.6840	0.0574	0.0489
	Model 2/5	83	21	106.8830	516.7665	0.0505	0.0474
	Model 3/5	83	21	104.6213	515.2294	0.0387	0.0467
	Model 4/5	83	21	104.4361	514.9662	0.0088	0.0467
	Model 5/5	84	20	109.3705	518.2067	0.0650	0.0482
	Optimum values for interaction parameters			104.4361	514.9662		
[MIM][SCN]	Model 1/5	45	11	181.1421	168.7088	0.0487	0.0488
	Model 2/5	45	11	183.8349	171.4511	0.0478	0.0487
	Model 3/5	45	11	186.7495	174.4316	0.0296	0.0487
	Model 4/5	45	11	183.8349	171.4511	0.0528	0.0487
	Model 5/5	44	12	183.8349	171.4511	0.0587	0.0487

Table 1. *Continued*

Main groups	Models	No. of data points in training set	No. of data points in validation set	α_{mn}	α_{nm}	RMSEA for validation set	RMSEA for all data
	Optimum values for interaction parameters			186.7495	174.4316		
[MIM][TFA]	Model 1/5	73	21	131.6600	154.4708	0.0404	0.0498
	Model 2/5	73	21	138.9052	148.7753	0.0108	0.0493
	Model 3/5	73	21	138.2013	147.9715	0.0623	0.0496
	Model 4/5	74	20	105.9965	178.9719	0.0493	0.0513
	Model 5/5	73	21	138.9052	148.7753	0.0666	0.0493
	Optimum values for interaction parameters			138.9052	148.7753		
[OCH_2MIM][Tf_2N]	Model 1/5	14	4	−603.6483	159.9201	0.0705	0.0597
	Model 2/5	15	3	−630.6696	152.2192	0.0498	0.0696
	Model 3/5	14	4	−603.6483	159.9201	0.0526	0.0618
	Model 4/5	14	4	−612.7348	157.2275	0.0444	0.0642
	Model 5/5	15	3	−603.6483	159.9201	0.1341	0.0597
	Optimum values for interaction parameters			−612.7348	157.2275		
[MPY][BF_4]	Model 1/5	17	4	24.4715	268.4828	0.0567	0.0542
	Model 2/5	17	4	23.2569	267.8702	0.0743	0.0537
	Model 3/5	16	5	23.2586	267.8666	0.0357	0.0537
	Model 4/5	17	4	25.8636	226.7528	0.0526	0.0495
	Model 5/5	17	4	24.4715	268.4828	0.0367	0.0542
	Optimum values for interaction parameters			23.2586	267.8666		
[MPY][Tf_2N]	Model 1/5	46	11	29.9099	73.5104	0.0164	0.0168
	Model 2/5	45	12	16.3630	61.9998	0.0143	0.0146
	Model 3/5	45	12	22.1635	66.9491	0.0152	0.0147
	Model 4/5	46	11	22.1651	66.9472	0.0136	0.0147
	Model 5/5	46	11	29.0407	72.7772	0.0205	0.0165
	Optimum values for interaction parameters			22.1651	66.9472		
[MPYR][Tf_2N]	Model 1/5	247	62	−140.3341	465.1145	0.0855	0.0902
	Model 2/5	247	62	−143.0034	442.1935	0.0777	0.0870
	Model 3/5	247	62	−134.3077	445.0594	0.0945	0.0899
	Model 4/5	248	61	−131.8377	445.8533	0.0970	0.0910
	Model 5/5	247	62	−136.5032	460.3062	0.0936	0.0911
	Optimum values for interaction parameters			−143.0034	442.1935		
[MPYR][TfO]	Model 1/5	45	11	116.4028	186.9445	0.0793	0.0568
	Model 2/5	45	11	204.0040	102.5842	0.0544	0.0547
	Model 3/5	44	12	203.1707	102.7460	0.0302	0.0548
	Model 4/5	45	11	201.7828	99.9781	0.0540	0.0560
	Model 5/5	45	11	201.5003	99.7521	0.0565	0.0561
	Optimum values for interaction parameters			203.1707	102.7460		
[N][Tf_2N]	Model 1/5	43	10	291.7498	−19.6023	0.1569	0.1381
	Model 2/5	42	11	286.3920	−25.9535	0.0785	0.1346
	Model 3/5	43	10	296.9503	−105.8313	0.0953	0.1120
	Model 4/5	42	11	333.7460	−43.4600	0.1658	0.1411
	Model 5/5	42	11	309.3349	5.9634	0.1661	0.1444
	Optimum values for interaction parameters			286.3920	−25.9535		
[P][Cl]	Model 1/5	62	15	204.8808	−275.3345	0.0927	0.0955
	Model 2/5	62	15	205.3366	−272.6423	0.1125	0.0953
	Model 3/5	62	15	204.2149	−273.6277	0.0839	0.0955
	Model 4/5	61	16	204.2149	−273.6277	0.0840	0.0955
	Model 5/5	61	16	208.0779	−272.8281	0.0944	0.0949
	Optimum values for interaction parameters			204.2149	−273.6277		
[P][$MeSO_4$]	Model 1/5	23	6	315.7386	546.6732	0.0200	0.0202
	Model 2/5	23	6	315.5255	547.0882	0.0232	0.0202
	Model 3/5	23	6	315.5689	547.0037	0.0163	0.0202
	Model 4/5	23	6	306.8708	542.5329	0.0212	0.0192
	Model 5/5	24	5	306.8776	542.5200	0.0165	0.0192
	Optimum values for interaction parameters			315.5689	547.0037		
[P][Tf_2N]	Model 1/5	174	44	238.4277	−170.4392	0.1461	0.1276
	Model 2/5	175	43	219.7043	−164.8520	0.1249	0.1255
	Model 3/5	174	44	209.6727	−160.0809	0.1341	0.1248
	Model 4/5	175	43	221.8450	−162.2714	0.1308	0.1263
	Model 5/5	174	44	220.2868	−176.8528	0.0889	0.1240
	Optimum values for interaction parameters			220.2868	−176.8528		

Results and Discussion

Prediction of the solubility of CO_2 in pure ILs at high temperatures

The comparison of experimental CO_2 solubility data with the calculated results by UNIFAC model is summarized in Table 2. Although we are aware that not all of the solubility data coming from literatures are fully trustable and even a few negative values at very low pressure are reported, which are denoted in red in Supporting Information, the calculated results by UNIFAC model are close to experimental data with the ARDs less than 20.0% for most of the IL—CO_2 systems. However, when the system pressure exceeds 500 bar, some large deviations between them will arise because in

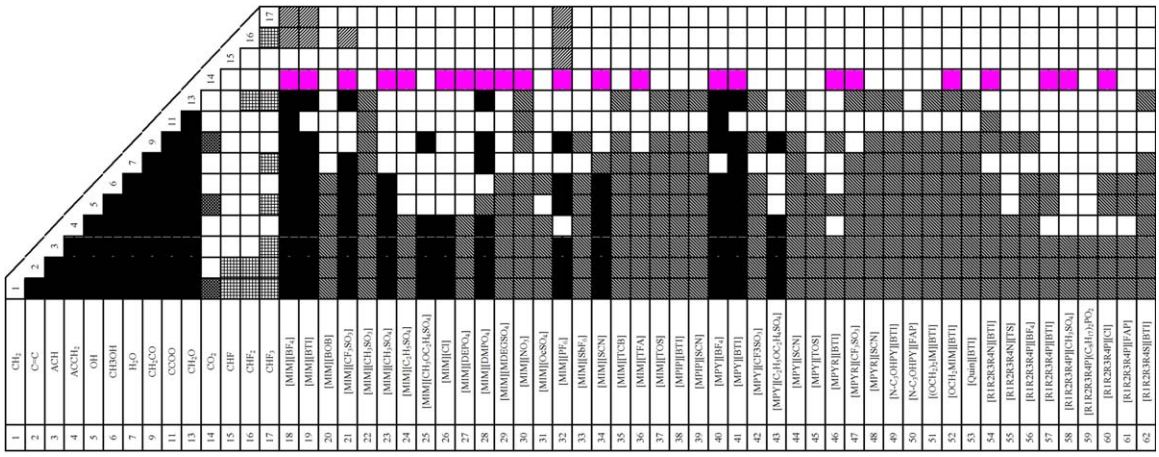

Figure 2. Current UNIFAC parameter matrix for ILs.

■ Previously published parameters;[43] ▨ previously published new parameters;[44] ▨ Previously published parameters;[63] ▦ Previously published parameters;[72] ▩ Previously published parameters;[64] □ New parameters(this work); ▢ No parameters available. [Color figure can be viewed in the online issue, which is available at wileyonlinelibrary.com.]

this case the calculated values are bigger than 1.0. This may be attributed to the unsuitability of Eq. 10 at very high-pressure region where one should use an equation of state. In this work, most of the collected experimental data at high temperatures (>273 K) were used to correlate the group interaction parameters, while some new solubility data published very recently[127,128] were used to cross-check the accuracy of UNFAC prediction at high temperatures. It was found that the relative deviations of CO_2 solubility between experimental data and predicted values are small, the ARDs being 8.8 2%, 4.28%, and 10.03% for $[OMIM]^+[Tf_2N]^-$, $[BMIM]^+[PF_6]^-$, and $[BMIM]^+[Tf_2N]^-$, respectively (see Supporting Information for detailed values). Moreover, it is noted that the uncertainty in the predicted solubility is a little higher at very low pressures. Therefore, the UNIFAC model with new group parameters obtained in this work can be applied for predicting the solubility of CO_2 in pure ILs at high temperatures (>273.15 K) and pressures below 500 bar.

Prediction of the solubility of CO_2 in ILs at low temperatures

The solubility data of CO_2 in two common ILs, i.e., $[OMIM]^+[BF_4]^-$ and $[OMIM]^+[Tf_2N]^-$, were measured at three low temperatures (273.2 K, 258.2 K, and 243.2 K) and pressures up to 25 bar, as shown in Figures 3 and 4, along with the predicted results by UNIFAC model. The detailed values are given in Supporting Information. It is observed that the solubility of CO_2 in $[OMIM]^+[Tf_2N]^-$ is higher than in $[OMIM]^+[BF_4]^-$ at the same operating conditions, exhibiting the same trend as that at high temperatures. Moreover, low temperature is favorable for increasing the CO_2 solubility significantly, and a high solubility at low temperatures will lower the viscosity of the mixture of IL and CO_2. In this work, we do not pay attention to the viscosity at low temperatures because our aim is to concentrate our efforts on measuring the solubility data and establishing the predictive UNIFAC model. However, we are aware of the importance of handling the viscosity problem, which should be addressed in the future work.

It can be seen that the UNIFAC predicted results are in good agreement with the experimental data at low temperatures, and the ARDs of CO_2 solubility in $[OMIM]^+[BF_4]^-$ and $[OMIM]^+[Tf_2N]^-$ are 2.51% and 3.29%, respectively, manifesting the applicability of UNIFAC model for predicting the CO_2 solubility in pure ILs from high to low temperatures.

Prediction of the solubility of CO_2 in the binary mixture of ILs

Two methods are examined to predict the solubility of CO_2 in the binary mixture of ILs at high or low temperatures. In Method one, we take the mole fraction average of individual ILs to account for CO_2 solubility according to the so-called lever rule

$$x_1 = X_2 x_{1,2} + X_3 x_{1,3} \tag{13}$$

where X_2 and X_3 are mole fractions of individual ILs in the mixed ILs on a CO_2-free basis ($X_2 + X_3 = 1.0$), and $x_{1,2}$ and $x_{1,3}$ are mole fractions (i.e., solubility) of CO_2 in pure ILs at the same temperature and pressure as in the mixed ILs, which can be well predicted by the UNIFAC model as described previously. In Method two, the binary interaction parameters between IL groups are assumed to be zero ($\alpha_{mn} = \alpha_{nm} = 0$) since they are electrically neutral groups and have the similar polarity.

The comparison of experimental solubility data[46] of CO_2 in $[EMIM]^+[BF_4]^-$, $[OMIM]^+[Tf_2N]^-$, and their mixtures, as well as CO_2 in $[BMIM]^+[BF_4]^-$, $[OMIM]^+[Tf_2N]^-$, and their mixtures, with the predicted results by UNIFAC model (including Method one and Method two) at high temperatures was made in this work (see Supporting Information). The ARDs of CO_2 solubility in the binary mixture of $[EMIM]^+[BF_4]^-$ and $[OMIM]^+[Tf_2N]^-$ for Method one and Method two are 22.17% and 13.21%, respectively, while in the binary mixture of $[BMIM]^+[BF_4]^-$ and $[OMIM]^+[Tf_2N]^-$, they are 21.04% and 13.72%, respectively.

The solubility data of CO_2 in the binary mixture of an equimolar amount of $[OMIM]^+[BF_4]^-$ and $[OMIM]^+[Tf_2N]^-$ were measured in this work at three low temperatures (273.2 K, 258.2 K, and 243.2 K) and pressures up to 25 bar. As shown in Figure 5, both Method one and Method two can predict the solubility of CO_2 in the binary mixture of ILs satisfactorily, the ARDs being 7.30% and

Table 2. Comparison of Experimental CO_2 Solubility in ILs with the Predicted Results by the UNIFAC Model

ILs	*T* range (K)	*P* range (bar)	ARD (%)	No. of data points	Refs.
$[BMIM]^+[BF_4]^-$	298.00–298.20	0.10–20.00	15.74	9	73
	293.15–383.15	10.50–246.00	9.46	59	74
	283.15–323.15	0.02–13.00	18.40	84	75
	303.38–344.27	0.22-0.92	37.22	11	76
	278.47–368.22	5.87–467.20	10.55	97	77
	282.75–348.15	0.10–20.00	14.96	36	78
	303.72–344.49	0.18-0.84	27.56	21	79
	298.15–298.15	6.50–60.70	7.21	7	80
	298.20–333.30	10.50–246.00	7.70	20	81
	307.55–322.15	6.50–60.70	9.56	40	82
	313.20–333.20	11.20–53.90	8.31	12	46
	298.20–333.20	8.29–47.86	3.54	23	14
		total ARD	13.23	419	
$[BMIM]^+[Cl]^-$	353.15–373.15	24.54–369.46	12.43	45	83
$[BMIM]^+[MDEGSO_4]^-$	313.31–333.36	14.30–91.20	45.70	11	84
$[BMIM]^+[MeSO_4]^-$	293.20–413.10	9.08–98.05	16.22	54	85
$[BMIM]^+[NO_3]^-$	313.15–333.15	15.47–93.17	27.58	21	1
	293.13–368.24	3.68–128.32	3.71	66	86
	298.20–333.20	10.31–93.16	5.62	17	81
		total ARD	8.84	104	
$[BMIM]^+[PF_6]^-$	298.00–298.20	0.11–20.00	15.27	9	73
	293.29–363.54	4.30–439.00	11.75	90	87
	293.15–393.15	1.05–96.85	13.35	43	88
	283.15–323.15	0.03–12.99	5.71	158	8
	283.15–323.15	0.00–13.00	6.09	160	75
	298.15–298.15	2.60-40.20	5.82	9	62
	283.15–343.04	0.41-0.92	37.98	14	89
	313.15–323.15	15.17–95.67	23.78	21	1
	282.05–348.25	0.10–20.00	13.05	36	78
	298.20–333.40	5.60–146.39	7.96	70	81
	297.56–322.52	7.90-80.80	3.96	42	90
	298.15–298.15	5.29-6.67	2.90	4	36
		total ARD	9.04	656	
$[BMIM]^+[SCN]^-$	292.35–384.15	10.50–315.00	13.95	56	74
$[BMIM]^+[Tf_2N]^-$	279.98–339.97	2.92-48.00	12.03	16	91
	293.35–344.55	10.70–428.00	10.95	84	92
	283.15–323.15	0.01–13.00	22.30	98	75
	283.36–343.78	0.68-1.12	8.10	14	93
	313.20–323.20	80.80–199.40	5.09	8	94
	292.65–363.26	6.29–499.90	12.89	68	95
	313.15–453.15	4.20–142.61	20.42	133	96
	298.10–333.30	11.38–132.43	8.89	55	81
		total ARD	15.82	476	
$[BMIM]^+[TFA]^-$	298.00–298.20	0.11–20.00	12.40	9	73
	298.17–333.41	11.70–92.60	6.95	19	84
	293.25–363.18	9.79–484.58	12.46	45	97
		total ARD	11.02	73	
$[BMIM]^+[TfO]^-$	303.20–343.20	2.15–65.21	23.57	35	98
	303.85–344.55	8.50–375.00	18.12	65	99
	298.20–333.30	10.44–114.77	14.47	27	81
		total ARD	18.84	127	
$[BMPYR]^+[TfO]^-$	303.15–373.25	18.80–482.10	9.81	59	100
$[BMPYR]^+[Tf_2N]^-$	303.78–344.15	0.49-0.57	50.50	11	101
	293.10–413.20	2.80–108.13	20.46	26	102
	283.15–323.15	0.02–13.00	32.33	72	75
	303.15–373.15	6.80–627.70	13.38	72	103
	313.20–323.20	80.60–200.60	5.17	8	94
		total ARD	23.38	189	
$[BPY]^+[BF_4]^-$	313.15–333.15	15.47–95.80	10.73	21	1
$[C_2OMIM]^+[Tf_2N]^-$	303.15–323.15	0.10-1.60	44.85	18	11
$[C_5MIM]^+[Tf_2N]^-$	293.30–363.29	6.18–598.05	7.10	144	104
$[DMIM]^+[Tf_2N]^-$	313.20–323.20	80.70–201.50	18.11	8	94
	313.15–313.15	20.00–144.00	26.32	14	105
	298.15–343.15	14.74–148.47	16.58	22	106
	298.15–343.15	14.74–148.47	16.58	22	107
		total ARD	18.83	66	
$[EMIM]^+[BF_4]^-$	303.20–343.20	4.96-43.29	23.37	25	108
	298.15–298.15	2.51-8.75	11.24	9	36
	298.20–313.20	5.30–40.60	8.79	17	109
	313.20–333.20	11.20–54.70	10.01	12	46
		total ARD	15.26	63	
$[EMIM]^+[DEPO_4]^-$	313.15–333.15	0.24-1.99	2.35	22	110
$[EMIM]^+[EtSO_4]^-$	303.20–343.20	2.11–49.62	10.16	35	98
	303.15–353.15	1.22-15.47	8.16	39	111

Table 2. *Continued*

ILs	*T* range (K)	*P* range (bar)	ARD (%)	No. of data points	Refs.
	313.15–333.15	14.36–94.61	16.14	21	[1]
		total ARD	10.66	95	
$[EMIM]^+[MDEGSO_4]^-$	303.20–343.20	8.54–67.10	3.94	30	[112]
$[EMIM]^+[PF_6]^-$	308.14–366.03	14.90–523.00	24.72	50	[113]
$[EMIM]^+[Tf_2N]^-$	297.90–298.20	0.50-20.00	11.28	9	[73]
	312.10–453.15	6.26–147.70	17.27	191	[114]
	292.75–344.55	12.20–432.00	12.67	78	[92]
	303.63–344.23	0.43-0.57	48.88	14	[101]
	303.63–344.23	0.43-0.57	48.88	14	[19]
	283.43–343.07	0.65-0.86	22.14	5	[93]
	292.16–363.55	6.20–478.50	7.04	153	[104]
	298.15–343.15	12.35–147.94	8.57	21	[106]
	298.15–343.15	12.35–147.94	8.57	21	[107]
	298.15–298.15	2.13-9.03	20.32	8	[36]
		total ARD	14.53	514	
$[EMIM]^+[TFA]^-$	298.10–298.10	0.10–20.00	9.90	9	[73]
	298.10–348.20	0.10–20.00	18.16	27	[48]
		total ARD	16.10	36	
$[EMIM]^+[TfO]^-$	303.20–343.20	1.80-58.84	8.47	30	[115]
	303.85–344.55	8.00–378.00	18.52	55	[99]
		total ARD	14.97	85	
$[HMIM]^+[BF_4]^-$	293.18–368.16	5.40–513.20	9.40	93	[116]
	298.15–298.15	3.12-8.99	6.51	8	[36]
	307.55–322.15	21.30–86.40	4.25	44	[82]
		total ARD	7.71	145	
$[HMIM]^+[PF_6]^-$	298.31–363.58	6.40–334.40	9.60	76	[117]
	298.15–298.15	2.96-9.27	14.71	14	[36]
		total ARD	10.39	90	
$[HMIM]^+[Tf_2N]^-$	297.30–297.40	0.09–19.75	9.98	9	[73]
	303.85–344.55	14.00–390.00	9.83	90	[92]
	293.15–413.20	6.01–99.11	20.22	25	[118]
	288.48–343.20	0.29-0.94	36.24	11	[119]
	281.90–348.60	0.09–19.76	14.08	72	[120]
	283.16–323.17	0.01–13.00	14.61	57	[84]
	278.12–368.44	4.22–143.37	11.32	123	[121]
	298.10–333.30	13.15–115.58	7.36	28	[81]
	298.15–343.15	8.00–247.08	11.12	26	[106]
	298.15–343.15	8.00–247.08	11.12	26	[107]
	298.15–298.15	1.57-8.40	24.61	10	[122]
	298.15–298.15	1.64-8.59	5.62	9	[36]
		total ARD	12.75	486	
$[HMIM]^+[TfO]^-$	313.23–313.39	14.94-84.23	11.51	6	[18]
	303.85–344.55	12.50–363.00	12.44	70	[99]
		total ARD	12.37	76	
$[HMMIM]^+[Tf_2N]^-$	298.20–333.30	14.97–118.04	13.21	29	[81]
$[HMPY]^+[Tf_2N]^-$	283.18–323.15	0.01–13.00	18.98	56	[84]
$[HMPYR]^+[Tf_2N]^-$	303.15–373.15	10.60–475.50	13.43	64	[123]
$[MMIM]^+[DMPO_4]^-$	313.15–333.15	0.49-1.75	0.017	12	[110]
$[N_{1,8,8,8}]^+[Tf_2N]^-$	313.20–323.20	80.80–205.60	28.55	8	[94]
$[N_{2,1,1,3}]^+[Tf_2N]^-$	313.22–313.25	11.34–94.66	7.44	8	[18]
$[N_{4,1,1,1}]^+[Tf_2N]^-$	282.93–343.07	0.36-0.89	41.51	12	[93]
	313.20–323.20	85.80–196.30	25.76	8	[94]
	333.23–333.23	15.60–80.90	14.55	6	[84]
		total ARD	30.44	26	
$[N_{4,4,4,1}]^+[Tf_2N]^-$	298.15–298.15	0.05-5.50	61.84	11	[75]
$[NMIM]^+[PF_6]^-$	293.15–298.15	8.60-35.40	10.67	11	[62]
$[OMIM]^+[BF_4]^-$	307.79–363.29	5.71–515.40	11.44	93	[124]
	313.15–333.15	15.61–93.73	12.12	21	[1]
	307.55–322.15	41.70–87.20	2.16	32	[82]
		total ARD	9.47	146	
$[OMIM]^+[PF_6]^-$	313.15–333.15	16.00–92.88	16.86	21	[1]
$[OMIM]^+[Tf_2N]^-$	303.15–353.15	1.12–20.63	28.54	42	[3]
	297.55–344.55	6.80–348.00	22.19	96	[92]
	298.20–333.30	13.26–114.69	10.58	22	[81]
	313.20–333.20	11.30–55.40	27.01	12	[46]
		total ARD	22.59	172	
$[OMIM]^+[TfO]^-$	303.85–344.55	6.80–340.00	9.86	65	[99]
$[OMPYR]^+[Tf_2N]^-$	303.15–373.15	5.10–359.20	19.94	72	[123]
$[P_{6,6,6,14}]^+[Cl]^-$	313.20–323.20	82.10–207.10	3.79	8	[94]
	302.55–363.68	1.68–245.70	13.23	69	[125]
		total ARD	12.25	77	
$[P_{1,4,4,4}]^+[MeSO_4]^-$	313.16–363.30	6.59–126.40	6.23	29	[126]
$[P_{6,6,6,14}]^+[Tf_2N]^-$	293.35–375.35	5.30–222.00	22.74	90	[100]
	313.20–323.20	80.90–201.70	5.20	8	[94]
	292.88–363.53	1.06–721.85	10.97	120	[125]
		total ARD	15.62	218	

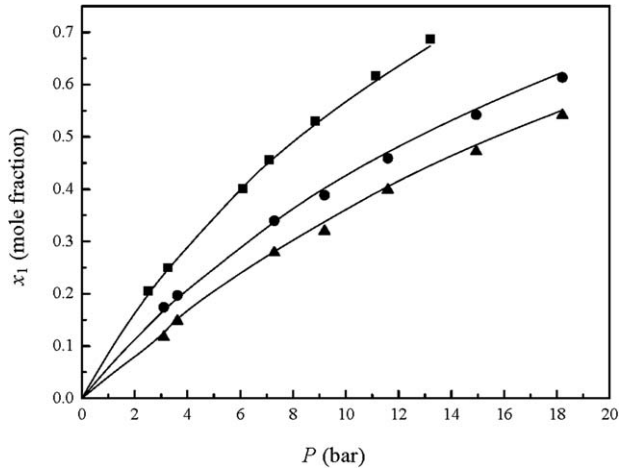

Figure 3. Solubility of CO_2 (1) in $[OMIM]^+[BF_4]^-$ (2) at low temperatures.

Solid lines, predicted results by the UNIFAC model; scattered points, experimental data. (■) 243.2 K; (•) 258.2 K; (▲) 273.2 K.

8.56%, respectively. This indicates that the application of UNIFAC model can be effectively extrapolated from single ILs to mixed ILs whether it is at high or low temperatures. However, as a whole, Method two seems more accurate for both at high and low temperatures.

Structure–property relation for the CO_2 solubility in ILs

The UNIFAC model can be used to identify the structure–property relation between molecular structure of IL and separation performance (e.g., CO_2 solubility). The Henry's law constants on the mole fraction scale provide an immediate evaluation of CO_2 solubility in various ILs, and can be obtained by

$$H(T,P)=\lim_{x_1\to 0}\gamma_1 P_1^s(T)=\gamma_1^{\infty}P_1^s(T) \tag{14}$$

where γ_1^{∞} is the activity coefficient of CO_2 in ILs at infinite dilution predicted by the UNIFAC model.

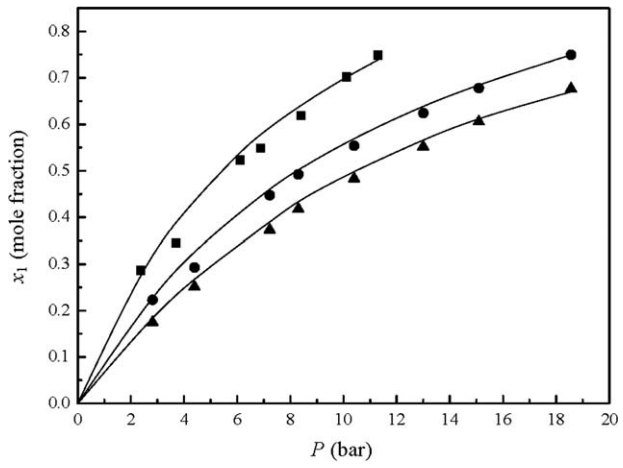

Figure 4. Solubility of CO_2 (1) in $[OMIM]^+[Tf_2N]^-$, (2) at low temperatures.

Solid lines, predicted results by the UNIFAC model; scattered points, experimental data. (■) 243.2 K; (•) 258.2 K; (▲) 273.2 K.

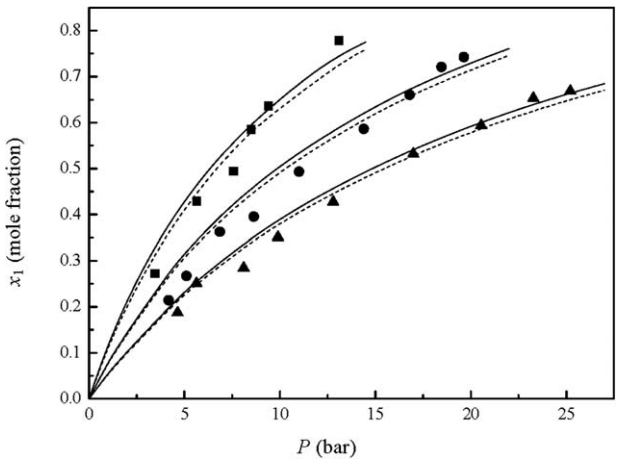

Figure 5. Solubility of CO_2 (1) in an equimolar amount of $[OMIM]^+[BF_4]^-$ and $[OMIM]^+[Tf_2N]^-$ at low temperatures.

Dashed lines, predicted results by Method one; Solid lines, predicted results by Method two; Scattered points, experimental data. (■) 243.2 K; (•) 258.2 K; (▲) 273.2 K.

Figure 6 shows the comparison of Henry's law constants of CO_2 in various ILs at 298.15 K exhaustively collected from literatures,[8,24,45,75,82,84,85,93,97,104,109–111,115,119,120,129–135] along with the predicted results by the UNIFAC model in increasing order. It can be seen that both agree well except for one experimental data marked with black circle, which may be caused by the experimental error or sample purity.

The influence of carbon number in the alkyl side-chain on the cation was further investigated by means of the UNIFAC model so as to find new structure–property relation for the CO_2 solubility in ILs. As shown in Figure 7, as the carbon number increases, the Henry's law constants tend to decrease for all ILs as expected. However, it was found that the decreasing slope is different for different ILs. For the ILs with the anions (e.g., $[BF_4]^-$, $[PF_6]^-$, and $[TfO]^-$) the Henry's law constants first decrease quickly and then slowly when the alkyl chain on the cation becomes longer, while for the ILs with the anions (e.g., $[Tf_2N]^-$), they always exhibit a slow decrease. In addition, we do recognize that some ILs with long alkyl chain may not actually exists at molten state at 298.15 K, but the similar trend is also predicted at higher temperatures by the UNIFAC model. Moreover, it is interesting to find that when the carbon number increases to a certain degree, the Henry's law constants approach a common asymptotic value for all of the ILs investigated around 2.0 MPa, which maybe the lowest limit for physical absorption with ILs at 298.15 K, independent of anion choice.

Conclusions

Although the UNIFAC model has already been widely used for predicting the thermodynamic behaviors of traditional organic solvents-CO_2 systems in the community of chemical engineering, it is the first work to extend the predictive model to IL—CO_2 systems, to the best of our knowledge. In this work, the new group binary interaction parameters (α_{mn} and α_{nm}) between CO_2 and 22 IL groups were obtained by means of correlating the solubility data at

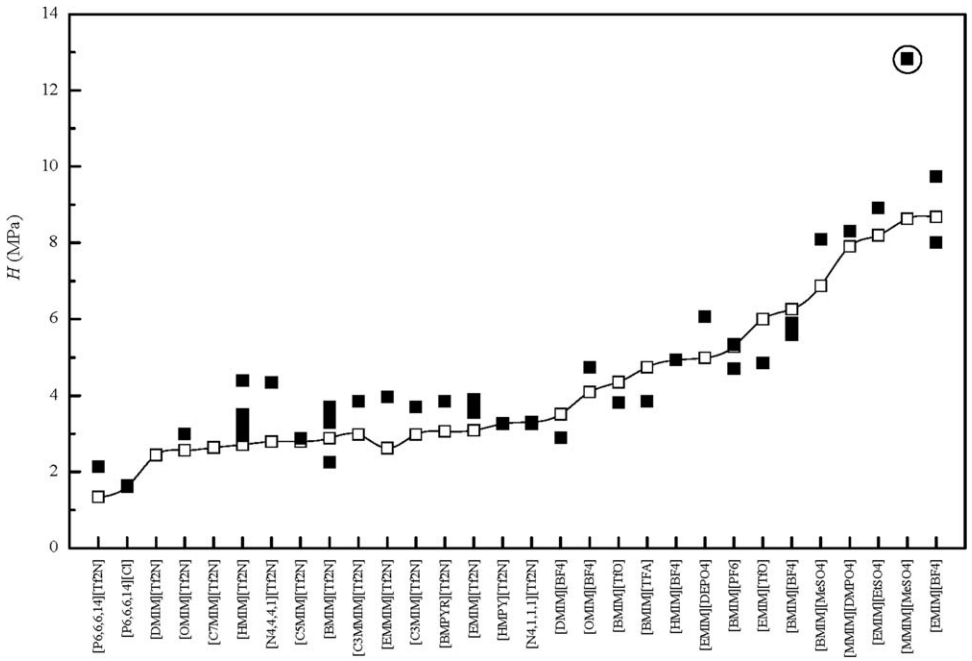

Figure 6. Henry's constants of CO_2 in various ILs at $T = 298.15$ K.

(■) Predicted results by the UNIFAC model; (■) Experimental results from literatures.[8,24,45,75,82,84,85,93,97,104,109–111,115,119,120,129–135.]

high temperatures. However, the UNIFAC model can be extended to predict the CO_2 solubility in pure ILs either at high (>273.2 K) or low temperatures (<273.2 K) effectively. Besides, two methods (Method one and Method two) based on the UNIFAC model were proposed to predict the solubility of CO_2 in the binary mixture of ILs, and Method two seems more suitable for either at high or low temperatures. This work demonstrates the applicability of UNIFAC model for IL—CO_2 system over a wider temperature and pressure (<500 bar) window. The previous structure–property relation that anion is the primary factor for dominating the CO_2 solubility in ILs is not supported by the UNIFAC model. The Henry's law constants for all of the ILs investigated approach a common asymptotic value, as the alkyl chain length on the cation becomes long enough.

It should be noted that the IL groups added to the current UNIFAC parameter matrix are limited to interact with CO_2 physically, and the chemical interaction between CO_2 and IL group (e.g., [MIM][Ac]) has not been considered yet, due to the vacancy of group interaction parameters between CH_2 and IL group. Therefore, more experimental data are needed to fill the gaps for the ILs chemically absorbing CO_2. Besides, the weakness of group contribution (e.g., isomeric molecules and proximity effect) also exists in the current UNIFAC model. Despite these problems, we are still encouraged to develop the UNIFAC model for ILs, due to its better prediction accuracy and shorter calculation time in comparison with the COSMO—RS model.

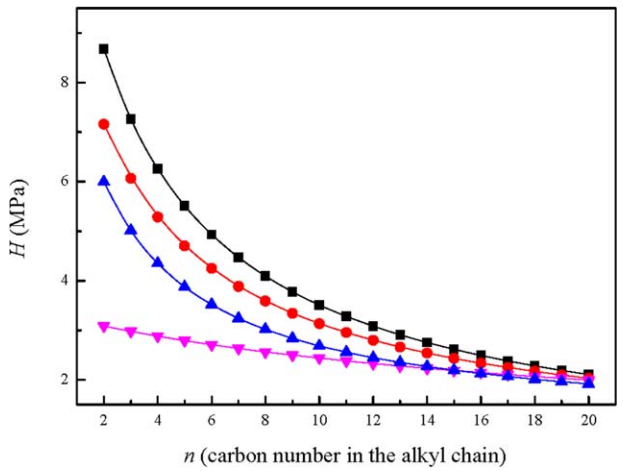

Figure 7. Henry's constants of CO_2 in $[R_nMIM]^+[X]^-$ families predicted by the UNIFAC model at $T = 298.15$ K.

(■) $[R_nMIM]^+[BF_4]^-$; (•) $[R_nMIM]^+[PF_6]^-$; (▲) $[R_nMIM]^+[TfO]^-$; (▼) $[R_nMIM]^+[Tf_2N]^-$.

[Color figure can be viewed in the online issue, which is available at wileyonlinelibrary.com.]

Acknowledgments

This work was financially supported by the National Nature Science Foundation of China under Grants (Nos. 21121064 and 21076008).

Literature Cited

1. Blanchard LA, Gu Z, Brennecke JF. High-pressure phase behavior of ionic liquid/CO_2 systems. *J Phys Chem B*. 2001;105:2437–2444.
2. Kodama D, Kanakubo M, Kokubo M, Ono T, Kawanami H, Yokoyama T, Nanjo H, Kato M. CO_2 absorption properties of Brønsted acid-base ionic liquid composed of N,N-dimethylformamide and bis(trifluoromethanesulfonyl)amide. *J Supercrit Fluids*. 2010;52:189–192.
3. Jalili A, Safavi M, Ghotbi C, Mehdizadeh A, Hosseini-Jenab M, Taghikhani V. Solubility of CO_2, H_2S, and their mixture in the ionic liquid 1-octyl-3-methylimidazolium bis(trifluoromethyl)sulfonylimide. *J Phys Chem B*. 2012;116:2758–2774.
4. Li M. Dynamics of CO_2 adsorption on sodium oxide promoted alumina in a packed-bed reactor. *Chem Eng Sci*. 2011;66:5938–5944.
5. http://uicgroupecho.wikispaces.com/file/view/B_0308e_Rectisol.pdf. Accessed October 24, 2013.

6. http://en.wikipedia.org/wiki/Rectisol. Accessed October 24, 2013.
7. Camper D, Becker C, Koval C, Noble R. Diffusion and solubility measurements in room temperature ionic liquids. *Ind Eng Chem Res*. 2006;45:445–450.
8. Anthony JL, Maginn EJ, Brennecke JF. Solubilities and thermodynamic properties of gases in the ionic liquid 1-*n*-butyl-3-methylimidazolium hexafluorophosphate. *J Phys Chem B*. 2002;106:7315–7320.
9. Blatha J, Christb M, Deublerb N, Hirtha T, Schiestel T. Gas solubilities in room temperature ionic liquids - Correlation between RTiL-molar mass and Henry's law constant. *Chem Eng J*. 2011;172:167–176.
10. Cabaco MI, Besnard M, Danten Y, Coutinho JAP. Solubility of CO_2 in 1-butyl-3-methyl- imidazolium-trifluoro acetate ionic liquid studied by Raman spectroscopy and DFT investigations. *J Phys Chem B*. 2011;115:3538–3550.
11. Sharma P, Choi SH, Park SD, Baek IH, Lee GS. Selective chemical separation of carbondioxide by ether functionalized imidazolium cation based ionic liquids. *Chem Eng J*. 2012;181-182:834–841.
12. Bara JE, Gabriel CJ, Lessmann S, Carlisle TK, Finotello A, Gin DL, Noble RD. Enhanced CO_2 separation selectivity in Oligo(ethylene glycol) functionalized room-temperature ionic liquids. *Ind Eng Chem Res*. 2007;46:5380–5386.
13. Aki SNVK, Scurto AM, Brennecke J F. Ternary phase behavior of ionic liquid (IL)-organic-CO_2 systems. *Ind Eng Chem Res*. 2006;45: 5574–5585.
14. Lei Z, Qi X, Zhu J, Li Q, Chen B. Solubility of CO_2 in acetone, 1-butyl-3-methylimidazolium tetrafluoroborate, and their mixtures. *J Chem Eng Data*. 2012;57:3458–3466.
15. Zhang Z, Wu W, Wang B, Chen J, Shen D, Han B. X. High-pressure phase behavior of CO_2/acetone/ionic liquid system. *J Supercrit Fluids*. 2007;40:1–6.
16. Kühne E, Perez E, Witkamp GJ, Peters CJ. Solute influence on the high-pressure phase equilibrium of ternary systems with carbon dioxide and an ionic liquid. *J Supercrit Fluids*. 2008;45:27–31.
17. Kühne E, Perez E, Witkamp GJ, Peters CJ. Fluid phase behaviour of the ternary system bmim[BF_4] + 1-(4-isobutylphenyl)-ethanol + carbon dioxide. *J Supercrit Fluids*. 2008;45:293–297.
18. Mellein BR, Brennecke JF. Characterization of the ability of CO_2 to act as an antisolvent for ionic liquid/organic mixtures. *J Phys Chem B*. 2007;111:4837–4843.
19. Hong G, Jacquemin J, Husson P, Costa Gomes MF, Deetlefs M, Nieuwenhuyzen M, Sheppard O, Hardacre C. Effect of acetonitrile on the solubility of carbon dioxide in 1-ethyl-3-methylimidazolium bis(trifluoromethylsulfonyl)amide. *Ind Eng Chem Res*. 2006;45: 8180–8188.
20. Ventura SPM, Pauly J, Daridon JL, da Silva JAL, Marrucho IM, Dias AMA, Coutinho JAP. High pressure solubility data of carbon dioxide in (tri-*iso*-butyl(methyl)phosphonium tosylate + water) systems. *J Chem Thermodyn*. 2008;40:1187–1192.
21. Goodrich BF, de la Fuente JC, Gurkan BE, Lopez ZK, Price EA, Huang Y, Brennecke JF. Effect of water and temperature on absorption of CO_2 by amine-functionalized anion-tethered ionic liquids. *J Phys Chem B*. 2011;115:9140–9150.
22. Taib M, Murugesan T. Solubilities of CO_2 in aqueous solutions of ionic liquids (ILs) and monoethanolamine (MEA) at pressures from 100 to 1600 kPa. *Chem Eng J*. 2012;181-182:56–62.
23. Vega LF, Vilaseca O, Llovell F, Andreu JS. Modeling ionic liquids and the solubility of gases in them: recent advances and perspectives. *Fluid Phase Equilib*. 2010;294:15–30.
24. Camper D, Scovazzo P, Koval C, Noble R. Gas solubilities in room-temperature ionic liquids. *Ind Eng Chem Res*. 2004;43:3049–3054.
25. Scovazzo P, Camper D, Kieft J, Poshusta J, Koval C, Noble R. Regular solution theory of CO_2 gas solubility in room-temperature ionic liquids. *Ind Eng Chem Res*. 2004;43:6855–6860.
26. Camper D, Becker C, Koval C, Noble R. Low pressure hydrocarbon solubility in room temperature ionic liquids containing imidazolium rings interpreted using regular solution theory. *Ind Eng Chem Res*. 2005;44:1928–1933.
27. Paduszyński K, Domańska U. Solubility of aliphatic hydrocarbons in piperidinium ionic liquids: Measurements and modeling in terms of perturbed-chain statistical associating fluid theory and nonrandom hydrogen-bonding theory. *J Phy Chem B*. 2011;115:12537–12548.
28. Chen Y, Mutelet F, Jaubert J-N. Modeling the solubility of carbon dioxide in imidazolium-based ionic liquids with the PC-SAFT equation of state. *J Phys Chem B*. 2012;116:14375–14388.
29. Vega LF, Jackson G. 20 Years of the SAFT equation of state - Recent advances and challenges symposium held in Bellaterra, Barcelona, 19–21 September 2010. *Fluid Phase Equilib*. 2011;306:1–3.
30. Ji X, Adidharma H. Thermodynamic modeling of CO_2 solubility in ionic liquid with heterosegmented statistical associating fluid theory. *Fluid Phase Equilib*. 2010;293:141–150.
31. Manan NA, Hardacre C, Jacquemin J, Rooney DR, Youngs TGA. Evaluation of gas solubility prediction in ionic liquids using COSMOthermX. *J Chem Eng Data*. 2009;54:2005–2022.
32. Palomar J, Gonzalez-Miquel M, Polo A, Rodriguez F. Understanding the physical absorption of CO_2 in ionic liquids using the COSMO-RS method. *Ind Eng Chem Res*. 2011;50:3452–3463.
33. Gonzalez-Miquel M, Talreja M, Ethier AL, Flack K, Switzer JR, Biddinger EJ, Pollet P, Palomar J, Rodriguez F, Eckert CA, Liotta CL. COSMO-RS studies: Structure−property relationships for CO_2 capture by reversible ionic liquids. *Ind Eng Chem Res*. 2012;51:16066–16073.
34. Valencia-Marquez D, Flores-Tlacuahuac A, Vasquez-Medrano R. Simultaneous optimal design of an extractive column and ionic liquid for the separation of bioethanol-water mixtures. *Ind Eng Chem Res*. 2012;51:5866–5880.
35. Chavez-Islas LM, Vasquez-Medrano R, Flores-Tlacuahuac A. Optimal synthesis of a high purity bioethanol distillation column using ionic liquids. *Ind Eng Chem Res*. 2011;50:5175–5190.
36. Kim Y, Choi W, Jang J, Yoo K, Lee C. Solubility measurement and prediction of carbon dioxide in ionic liquids. *Fluid Phase Equilib*. 2005;228-229:439–445.
37. Jorgensen SS, Kolbe B, Gmehling J, Rasmussen P. Vapor-liquid equilibria by UNIFAC group contribution. *Ind Eng Chem Process Des Dev*. 1979;18:714–722.
38. Gmehling J, Rasmussen P, Fredenslund A. Vapor-liquid equilibria by UNIFAC group contribution. *2. Revision and extension*. *Ind Eng Chem Process Des Dev*. 1982;21:118–127.
39. Macedo EA, Weidlich U, Gmehling J, Rasmussen P. Vapor-liquid equilibria by UNIFAC group contribution. 3. Revision and extension. *Ind Eng Chem Process Des Dev*. 1983;22:676–678.
40. Tiegs D, Gmehling J, Rasmussen P, Fredenslund A. Vapor-liquid equilibria by UNIFAC group contribution. 4. Revision and extension. *Ind Eng Chem Res*. 1987;26:159–161.
41. Hansen HK, Rasmussen P, Fredenslund A, Schiller M, Gmehling J. Vapor-liquid equilibria by UNIFAC group contribution. 5. Revision and extension. *Ind Eng Chem Res*. 1991;30:2352–2355.
42. Wittig R, Lohmann J, Gmehling J. Vapor-liquid equilibria by UNIFAC group contribution. 6. Revision and extension. *Ind Eng Chem Res*. 2003;42:183–188.
43. Lei Z, Zhang J, Li Q, Chen B. UNIFAC model for ionic liquids. *Ind Eng Chem Res*. 2009;48:2697–2704.
44. Lei Z, Dai C, Liu X, Xiao L, Chen B. Extension of the UNIFAC model for ionic liquids. *Ind Eng Chem Res*. 2012;51:12135–12144.
45. Baltus RE, Culbertson BH, Dai S, Luo H, DePaoli DW. The low pressure solubility of CO_2 in room temperature ionic liquids measured with a quartz crystal microbalance. *J Phys Chem B*. 2004;108: 721–727.
46. Lei Z, Han J, Zhang B, Li Q, Zhu J, Chen B. Solubility of CO_2 in binary mixtures of room-temperature ionic liquids at high pressures. *J Chem Eng Data*. 2012;57:2153–2159.
47. Finotello A, Bara J, Narayan S, Camper D, Nobel R. Ideal gas solubilities and solubility selectivities in a binary mixture of room-temperature ionic liquids. *J Phys Chem B*. 2008;112:2335–2339.
48. Shiflett MB, Yokozeki A. Phase behavior of carbon dioxide in ionic liquids: [emim][acetate], [emim][trifluoroacetate], and [emim][acetate] + [emim][trifluoroacetate]. *J Chem Eng Data*. 2009;54:108–114.
49. Paduszyński K, Domańska U. A new group contribution method for prediction of density of pure ionic liquids over a wide range of temperature and pressure. *Ind Eng Chem Res*. 2012;51:591–604.
50. Zellner M, Claitor L, Prausnitz JM. Prediction of vapor-liquid equilibria and enthalpies of mixtures at low temperatures. *Ind Eng Chem Res*. 1970;9:549–564.
51. Canongia Lopes JN, Cordeiro TC, Esperança JMSS, Guedes HJR, Huq S, Rebelo LPN, Seddon KR. Deviations from ideality in mixtures of two ionic liquids containing a common ion. *J Phys Chem B*. 2005;109:3519–3525.
52. Fredenslund A, Jones RL, Pransnitz JM. Group contribution estimation of activity coefficients in nonideal liquid mixture. *AIChE J*. 1975;27:1086–1099.
53. Santiago RS, Santos GR, Aznar M. Liquid-liquid equilibrium in ternary ionic liquid systems by UNIFAC: New volume, surface area and interaction parameters. Part I. *Fluid Phase Equilib*. 2010;295:93–97.
54. Santiago RS, Aznar M. Liquid-liquid equilibrium in ternary ionic liquid systems by UNIFAC: New volume, surface area and interaction parameters. Part II. *Fluid Phase Equilib*. 2011;303:111–114.

55. Alevizou EI, Pappa GD, Voutsas EC. Prediction of phase equilibrium in mixtures containing ionic liquids using UNIFAC. *Fluid Phase Equilib.* 2009;284:99–105.
56. Nebig S, Bolts R, Gmehling J. Measurement of vapor-liquid equilibria (VLE) and excess enthalpies (H^E) of binary systems with 1-alkyl-3-methylimidazolium bis(trifluoromethylsulfonyl)imide and prediction of these properties and γ^∞ using modified UNIFAC (Dortmund). *Fluid Phase Equilib.* 2007;258:168–178.
57. Nebig S, Gmehling J. Measurements of different thermodynamic properties of systems containing ionic liquids and correlation of these properties using modified UNIFAC. *Fluid Phase Equilib.* 2010;294:206–212.
58. Nebig S, Liebert V, Gmehling J. Measurement and prediction of activity coefficients at infinite dilution (γ^∞), vapor-liquid equilibria (VLE) and excess enthalpies (H^E) of binary systems with 1,1-dialkyl-pyrrolidinium bis(trifluoromethylsulfonyl)imide using mod. UNIFAC (Dortmund). *Fluid Phase Equilib.* 2009;277:61–67.
59. Lei Z, Chen B, Li C, Liu H. Predictive molecular thermodynamic models for liquid solvents, solid salts, polymers, and ionic liquids. *Chem Rev.* 2008;108:1419–1455.
60. Breure B, Bottini SB, Witkamp GJ, Peters CJ. Thermodynamic modeling of the phase behavior of binary systems of ionic liquids and carbon dioxide with the group contribution equation of state. *J Phys Chem B.* 2007;111:14265–14270.
61. Bermejo MD, Martin A, Foco G, Cocero MJ, Bottini SB, Peters CJ. Application of a group contribution equation of state for the thermdynamic modeling of the binary systems CO_2 − 1-butyl-3-methyl imidazolium nitrate and CO_2 − 1-hydroxyl-1-methyl imidazolium nitrate. *J Supercrit Fluids.* 2009;50:112–117.
62. Kim JE, Lim JS, Kang JW. Measurement and correlation of solubility of carbon dioxide in 1-alkyl-3-methylimidazolium hexafluorophosphate ionic liquids. *Fluid Phase Equilib.* 2011;306:251–255.
63. Dong L, Zheng D, Wu X. Working pair selection of compression and absorption hybrid cycles through predicting the activity coefficients of hydrofluorocarbon + ionic liquid systems by the UNIFAC model. *Ind Eng Chem Res.* 2012;51:4741–4747.
64. Sander B, Skjold-Jørgensen S, Rasmussen P. Gas solubility calculations. *1. UNIFAC. Fluid Phase Equilib.* 1983;11:105–126.
65. Bondi A. Van der Waals volumes and radii. *J Phys Chem.* 1964;68: 441–451.
66. Nocon G, Weidlich U, Gmehling J, Menke J, Onken U. Prediction of gas solubilities by a modified UNIFAC equation. *Fluid Phase Equilib.* 1983;13:381–392.
67. Span R, Wagner W. A new equation of state for carbon dioxide covering the fluid region from the triple-point temperature to 1100 K at pressures up to 800 MPa. *J Phys Chem Ref Data.* 1996;25:1509–1596.
68. Shiflett MB, Yokozeki A. Solubility and diffusivity of hydrofluorocarbons in room-temperature ionic liquids. *AIChE J.* 2006;52:1205–1219.
69. Blanchard LA, Hancu D, Beckman EJ, Brennecke JF. Green processing using ionic liquids and CO_2. *Nature.* 1999;399:28–29.
70. MacCallum RC, Browne MW, Sugawara HM. Power analysis and determination of sample size for covariance structure modeling. *Psychol Meth.* 1996;1:130–149.
71. David A. Kenny. Measuring Model Fit. Available at: http://davidakenny.net/cm/fit.htm. Accessed October 24, 2013.
72. Kleiber M. An extension to the UNIFAC group assignment for prediction of vapor-liquid equilibria of mixtures containing refrigerants. *Fluid Phase Equilib.* 1995;107:161–188.
73. Yokozeki A, Shiflett MB, Junk CP, Grieco LM, Foo T. Physical and chemical absorptions of carbon dioxide in room-temperature ionic liquids. *J Phys Chem B.* 2008;112:16654–16663.
74. Revelli AL, Mutelet F, Jaubert JN. High carbon dioxide solubilities in imidazolium-based ionic liquids and in poly(ethylene glycol) dimethyl ether. *J Phys Chem B.* 2010;114:12908–12913.
75. Anthony JL, Anderson JL, Maginn EJ, Brennecke JF. Anion effects on gas solubility in ionic liquids. *J Phys Chem B.* 2005;109:6366–6374.
76. Jacquemin J, Costa Gomes MF, Husson P, Majer V. Solubility of carbon dioxide, ethane, methane, oxygen, nitrogen, hydrogen, argon, and carbon monoxide in 1-butyl-3-methylimidazolium tetrafluoroborate between temperatures 283 K and 343 K and at pressures close to atmospheric. *J Chem Thermodyn.* 2006;38:490–502.
77. Kroon MC, Shariati A, Costantini M, van Spronsen J, Witkamp GJ, Sheldon RA, Peters CJ. High-pressure phase behavior of systems with ionic liquids: Part V. The binary system carbon dioxide + 1-butyl-3-methylimidazolium tetrafluoroborate. *J Chem Eng Data.* 2005;50:173–176.
78. Shiflett MB, Yokozeki A. Solubilities and diffusivities of carbon dioxide in ionic liquids: [bmim][PF_6] and [bmim][BF_4]. *Ind Eng Chem Res.* 2005;44:4453–4464.
79. Husson-Borg P, Majer V, Costa Gomes, MF. Solubilities of oxygen and carbon dioxide in butyl methyl imidazolium tetrafluoroborate as a function of temperature and at pressures close to atmospheric pressure. *J Chem Eng Data.* 2003;48:480–485.
80. Tian S, Hou Y, Wu W, Ren S, Pang K. Physical properties of 1-butyl-3-methylimidazolium tetrafluoroborate/*N*-methyl-2-pyrrolidone mixtures and the solubility of CO_2 in the system at elevated pressures. *J Chem Eng Data.* 2012;57:756–763.
81. Aki SNVK, Mellein BR, Saurer EM, Brennecke JF. High-pressure phase behavior of carbon dioxide with imidazolium-based ionic liquids. *J Phys Chem B.* 2004;108:20355–20365.
82. Chen Y, Zhang S, Yuan X, Zhang Y, Zhang X, Dai W, Mori R. Solubility of CO_2 in imidazolium-based tetrafluoroborate ionic liquids. *Thermochim Acta.* 2006;441:42–44.
83. Jang S, Cho DW, Im T, Kim H. High-pressure phase behavior of CO_2 + 1-butyl-3-methylimidazolium chloride system. *Fluid Phase Equilib.* 2010;299:216–221.
84. Muldoon MJ, Aki SNVK, Anderson JL, Dixon JK, Brennecke JF. Improving carbon dioxide solubility in ionic liquids. *J Phys Chem B.* 2007;111:9001–9009.
85. Kumełan J, Tuma D, Maurer G. Solubility of CO_2 in the ionic liquids [bmim][CH_3SO_4] and [bmim][PF_6]. *J Chem Eng Data.* 2006; 51:1802–1807.
86. Bermejo MD, Montero M, Saez E, Florusse LJ, Kotlewska AJ, Cocero MJ, van Rantwijk F, Peters CJ. Liquid-vapor equilibrium of the systems butylmethylimidazolium nitrate-CO_2 and hydroxypropylmethylimidazolium nitrate-CO_2 at high pressure: Influence of water on the phase behavior. *J Phys Chem B.* 2008;112:13532–13541.
87. Shariati A, Gutkowski K, Peters CJ. Comparison of the phase behavior of some selected binary systems with ionic liquids. *AIChE J.* 2005;51:1532–1540.
88. Kamps ÁP, Tuma D, Xia J, Maurer G. Solubility of CO_2 in the ionic liquid [bmim][PF_6]. *J Chem Eng Data.* 2003;48:746–749.
89. Jacquemin J, Husson P, Majer V, Gomes MFC. Low-pressure solubilities and thermodynamics of solvation of eight gases in 1-butyl-3-methylimidazolium hexafluorophosphate. *Fluid Phase Equilib.* 2006; 240:87–95.
90. Zhang S, Yuan X, Chen Y, Zhang X. Solubilities of CO_2 in 1-butyl-3-methylimidazolium hexafluorophosphate and 1,1,3,3-tetramethylguanidium lactate at elevated pressures. *J Chem Eng Data.* 2005;50: 1582–1585.
91. Lee BC, Outcalt SL. Solubilities of gases in the ionic liquid 1-*n*-butyl-3-methylimidazolium bis(trifluoromethylsulfonyl)imide. *J Chem Eng Data.* 2006;51:892–897.
92. Shin EK, Lee BC, Lim JS. High-pressure solubilities of carbon dioxide in ionic liquids: 1-alkyl-3-methylimidazolium bis(trifluoromethylsulfonyl)imide. *J Supercrit Fluids.* 2008;45:282–292.
93. Jacquemin J, Husson P, Majer V, Costa Gomes M. Influence of the cation on the solubility of CO_2 and H_2 in ionic liquids based on the bis(trifluoromethylsulfonyl)imide anion. *J Solution Chem.* 2007;36: 967–979.
94. Manic MS, Queimada AJ, Macedo EA, Najdanovic-Visak V. High-pressure solubilities of carbon dioxide in ionic liquids based on bis(trifluoromethylsulfonyl)imide and chloride. *J Supercrit Fluids.* 2012;65:1–10.
95. Carvalho PJ, Álvarez VH, Marrucho IM, Aznar M, Coutinho JAP. High pressure phase behavior of carbon dioxide in 1-butyl-3-methylimidazolium bis(trifluoromethylsulfonyl)imide and 1-butyl-3-methylimidazolium dicyanamide ionic liquids. *J Supercrit Fluids.* 2009;50:105–111.
96. Raeissi S, Peters CJ. Carbon dioxide solubility in the homologous 1-alkyl-3-methylimidazolium bis(trifluoromethylsulfonyl)imide family. *J Chem Eng Data.* 2009;54:382–386.
97. Carvalho PJ, Alvarez VH, Schröder B, Gil AM, Marrucho IM, Aznar M, Santos LMNBF, Coutinho JAP. Specific solvation interactions of CO_2 on acetate and trifluoroacetate imidazolium based ionic liquids at high pressures. *J Phys Chem B.* 2009;113:6803–6812.
98. Soriano AN, Doma Jr. BT, Li MH. Carbon dioxide solubility in some ionic liquids at moderate pressures. *J Taiwan Inst Chem E.* 2009;40:387–393.
99. Shin EK, Lee BC. High-pressure phase behavior of carbon dioxide with ionic liquids: 1-alkyl-3-methylimidazolium trifluoromethanesulfonate. *J Chem Eng Data.* 2008;53:2728–2734.

100. Song HN, Lee B-C, Lim JS. Measurement of CO_2 solubility in ionic liquids: [BMP][TfO] and $[P_{14,6,6,6}][Tf_2N]$ by measuring bubble-point pressure. *J Chem Eng Data*. 2010;55:891–896.
101. Hong G, Jacquemin J, Deetlefs M, Hardacre C, Husson P, Costa Gomes MF. Solubility of carbon dioxide and ethane in three ionic liquids based on the bis{(trifluoromethyl)sulfonyl}imide anion. *Fluid Phase Equilib*. 2007;257:27–34.
102. Kumełan J, Tuma D, Kamps ÁP, Maurer G. Solubility of the single gases carbon dioxide and hydrogen in the ionic liquid [bmpy][Tf_2N]. *J Chem Eng Data*. 2010;55:165–172.
103. Yim JH, Song HN, Yoo KP, Lim JS. Measurement of CO_2 solubility in ionic liquids: [BMP][Tf_2N] and [BMP][$MeSO_4$] by measuring bubble-point pressure. *J Chem Eng Data*. 2011;56:1197–1203.
104. Carvalho PJ, Álvarez VH, Machado JJB, Pauly J, Daridon JL, Marrucho IM, Aznar M, Coutinho JAP. High pressure phase behavior of carbon dioxide in 1-alkyl-3-methylimidazolium bis(trifluoromethylsulfonyl)imide ionic liquids. *J Supercrit Fluids*. 2009;48:99–107.
105. Bogel-Łukasik R, Matkowska D, Bogel-Łukasik E, Hofman T. Isothermal vapour-liquid equilibria in the binary and ternary systems consisting of an ionic liquid, 1-propanol and CO_2. *Fluid Phase Equilib*. 2010;293:168–174.
106. Ren W, Sensenich B, Scurto AM. High-pressure phase equilibria of {carbon dioxide (CO_2) + *n*-alkyl-imidazolium bis(trifluoromethylsulfonyl)amide} ionic liquids. *J Chem Thermodyn*. 2010;42:305–311.
107. Ren W. High-Pressure Phase Equilibria of Ionic Liquids and Compressed Gases for Applications in Reactions and Absorption Refrigeration [PhD]. University of Kansas, KS: Chemical and Petroleum Engineering; 2009.
108. Soriano AN, Doma BT, Li MH. Solubility of carbon dioxide in 1-ethyl-3-methylimidazolium tetrafluoroborate. *J Chem Eng Data*. 2008;53:2550–2555.
109. Lei Z, Yuan J, Zhu J. Solubility of CO_2 in propanone, 1-ethyl-3-methylimidazolium tetrafluoroborate, and their mixtures. *J Chem Eng Data*. 2010;55:4190–4194.
110. Palgunadi J, Kang JE, Nguyen DQ, Kim JH, Min BK, Lee SD, Kim H, Kim HS. Solubility of CO_2 in dialkylimidazolium dialkylphosphate ionic liquids. *Thermochim Acta*. 2009;494:94–98.
111. Jalili AH, Mehdizadeh A, Shokouhi M, Ahmadi AN, Hosseini-Jenab M, Fateminassab F. Solubility and diffusion of CO_2 and H_2S in the ionic liquid 1-ethyl-3-methylimidazolium ethylsulfate. *J Chem Thermodyn*. 2010;42:1298–1303.
112. Soriano AN, Doma Jr. BT, Li MH. Solubility of carbon dioxide in 1-ethyl-3-methylimidazolium 2-(2-methoxyethoxy) ethylsulfate. *J Chem Thermodyn*. 2008;40:1654–1660.
113. Shariati A, Peters CJ. High-pressure phase behavior of systems with ionic liquids: II. The binary system carbon dioxide + 1-ethyl-3-methylimidazolium hexafluorophosphate. *J Supercrit Fluids*. 2004;29:43–48.
114. Schilderman AM, Raeissi S, Peters CJ. Solubility of carbon dioxide in the ionic liquid 1-ethyl-3-methylimidazolium bis(trifluoromethylsulfonyl)imide. *Fluid Phase Equilib*. 2007;260:19–22.
115. Soriano AN, Doma Jr. BT, Li MH. Carbon dioxide solubility in 1-ethyl-3-methylimidazolium trifluoromethanesulfonate. *J Chem Thermodyn*. 2009;41:525–529.
116. Costantini M, Toussaint VA, Shariati A, Peters CJ, Kikic I. High-pressure phase behavior of systems with ionic liquids: Part iv. Binary system carbon dioxide + 1-hexyl-3-methylimidazolium tetrafluoroborate. *J Chem Eng Data*. 2005;50:52–55.
117. Shariati A, Peters CJ. High-pressure phase behavior of systems with ionic liquids: Part III. The binary system carbon dioxide + 1-hexyl-3-methylimidazolium hexafluorophosphate. *J Supercrit Fluids*. 2004;30:139–144.
118. Kumełan J, Pérez-Salado Kamps Á, Tuma D, Maurer G. Solubility of CO_2 in the ionic liquid [hmim][Tf_2N]. *J Chem Thermodyn*. 2006;38:1396–1401.
119. Costa Gomes MF. Low-pressure solubility and thermodynamics of solvation of carbon dioxide, ethane, and hydrogen in 1-hexyl-3-methylimidazolium bis(trifluoromethylsulfonyl)amide between temperatures of 283 K and 343 K. *J Chem Eng Data*. 2007;52:472–475.
120. Shiflett MB, Yokozeki A. Solubility of CO_2 in room temperature ionic liquid [hmim][Tf_2N]. *J Phys Chem B*. 2007;111:2070–2074.
121. Raeissi S, Florusse L, Peters CJ. Scott-van Konynenburg phase diagram of carbon dioxide + alkylimidazolium-based ionic liquids. *J Supercrit Fluids*. 2010;55:825–832.
122. Kim YS, Jang JH, Lim BD, Kang JW, Lee CS. Solubility of mixed gases containing carbon dioxide in ionic liquids: measurements and predictions. *Fluid Phase Equilib*. 2007;256:70–74.
123. Yim JH, Song HN, Lee BC, Lim JS. High-pressure phase behavior of binary mixtures containing ionic liquid [HMP][Tf_2N], [OMP][Tf_2N] and carbon dioxide. *Fluid Phase Equilib*. 2011;308:147–152.
124. Gutkowski KI, Shariati A, Peters CJ. High-pressure phase behavior of the binary ionic liquid system 1-octyl-3-methylimidazolium tetrafluoroborate + carbon dioxide. *J Supercrit Fluids*. 2006;39:187–191.
125. Carvalho PJ, Álvarez VH, Marrucho IM, Aznar M, Coutinho JAP. High carbon dioxide solubilities in trihexyltetradecylphosphonium-based ionic liquids. *J Supercriti Fluids*. 2010;52:258–265.
126. Ramdin M, Vlugt TJH, de Loos TW. Solubility of CO_2 in the Ionic Liquids [TBMN][$MeSO_4$] and [TBMP][$MeSO_4$]. *J Chem Eng Data*. 2012;57:2275–2280.
127. Lei Z, Zhang B, Zhu J, Gong W, Lv J, Li Y. Solubility of CO_2 in methanol, 1-octyl-3-methylimidazolium bis(trifluoromethylsulfonyl)imide, and their mixtures. *Chinese J Chem Eng*. 2013;21:310–317.
128. Gonzalez-Miquel M, Bedia J, Abrusci C, Palomar J, Rodriguez F. Anion effects on kinetics and thermodynamics of CO_2 absorption in ionic liquids. *J Phy Chem B*. 2013;117:3398–3406.
129. Camper D, Bara J, Koval C, Noble R. Bulk-fluid solubility and membrane feasibility of Rmim-based room-temperature ionic liquids. *Ind Eng Chem Res*. 2006;45:6279–6283.
130. Zhang J, Zhang Q, Qiao B, Deng U. Solubilities of the gaseous and liquid solutes and their thermodynamics of solubilization in the novel room-temperature ionic liquids at infinite dilution by gas chromatography. *J Chem Eng Data*. 2007;52:2277–2283.
131. Hou Y, Baltus RE. Experimental measurement of the solubility and diffusivity of CO_2 in room-temperature ionic liquids using a transient thin-liquid-film method. *Ind Eng Chem Res*. 2007;46:8166–8175.
132. Urukova I, Vorholz J, Maurer G. Solubility of CO_2, CO, and H_2 in the ionic liquid [bmim][PF_6] from Monte Carlo. *J Phys Chem B*. 2005;109:12154–12159.
133. Kerlé D, Ludwig R, Geiger A, Paschek D. Temperature dependence of the solubility of carbon dioxide in imidazolium-based ionic liquids. *J Phys Chem B*. 2009;113:12727–12735.
134. Finotello A, Bara J, Camper D, Noble R. Room-temperature ionic liquids: temperature dependence of gas solubility selectivity. *Ind Eng Chem Res*. 2008;47:3453–3459.
135. Kerlé D, Ludwig R, Geiger A, Paschek D. Temperature dependence of the solubility of carbon dioxide in imidazolium-based ionic liquids. *J Phys Chem B*. 2009;113:12727–12735.

Manuscript received Nov. 28, 2012, and revision received Oct. 25, 2013.